# Effect of modification substrate on the microstructure of hydroxyapatite coating

# Effect of modification substrate on the microstructure of hydroxyapatite coating

**J Realpe-Jaramillo[1], J A Morales-Morales[1], J A González-Sánchez[2], R Cabanzo[3], E Mejía-Ospino[3] and J Rodríguez–Pereira[3]**
[1] Universidad Santiago de Cali, Cali, Colombia
[2] Universidad Autónoma de Campeche, Campeche, México
[3] Universidad Industrial de Santander, Bucaramanga, Colombia

E mail: jim.ale.mor@gmail.com

**Abstract**. Bioactive hydroxyapatite (HA) coatings were fabricated by a precipitation, sol-gel and dip-coating method. The effects of the aging time and the base used to adjust pH and substrate materials on the phases and microstructures of HA coatings were studied by field emission scanning electron microscopy FESEM, energy dispersive spectroscopy EDS, X-ray photoelectron spectroscopy XPS, and the vibrations of the phosphate groups were determined by Raman spectroscopy. The results showed that all the films were composed of the phases of $TiO_2$ and HA. With coated titanium substrate with $TiO_2$, the crystallinity of the HA coating increases, the structure became more compact and the Ca/P ratio increased because of the loss of P in the films. The addition of sodium hydroxide (adjusting the pH level to about 10) can increase the HA content in the coating. XPS and EDS results for steel substrate and titanium showed poor calcium content as obtained with a Ca/P ratio of 1.38 and 1.58, respectively, composition is similar to that of natural apatite. However, spectroscopic results suggest the presence of a mixture of hydroxyapatite and octacalcium phosphate. The different substrate materials have a high influence on the microstructure of the separated double films. However, hydroxyapatite nanopowders coatings were obtained using a simple method, with potential biomedical applications.

## 1. Introduction

Bioactive materials based on Hydroxyapatite (HA) have been widely used in hard tissue applications, such as implant coatings [1,2] and bone replacements [3,4], due to its stability in vivo conditions and its osteoconductivity. HA $[Ca_{10}(PO_4)_6(OH)_2]$ is a biocompatible and bioactive ceramic material capable of interacting and chemical bond formation with surrounding bone. However, it can not be directly used for implant devices because of its brittleness and strength limitations and hence a great deal of research is dedicated to the development of HA coatings and composites [5,6].

Growing research for development of HA coatings has led to the introduction of some strategy as the use of titanium oxide coatings, layered coatings HA/$TiO_2$ and $TiO_2$ nanotubes obtained by anodic oxidation on Ti substrates. In this study, the effects of substrate modification on the microstructure of HA coatings were investigated.

## 2. Material and methods

### *2.1. Synthesis of coatings hydroxyapatite nanopowders*

It began with surface preparation of rectangular plates of 304 stainless steel and Ti respectively, with dimensions of 2.0 and 4.0cm by 0.5mm thick. The polished plates were degreased, washed and dried at room temperature. Then an inorganic coating synthesis of $TiO_2$ by the sol-gel method was performed. For it is required a 100mL vessel which was added 16mL of ethanol ($CH_3CH_2OH$, EtOH, reagent grade, Sigma-Aldrich) and 1mL of acetyl acetone (Acach) as complexing agent. It was allowed to stir the solution after 15 minutes. 3.5mL of titanium butoxide ($(Ti(O(CH_2)_3CH_3))_4$), BuTi, Sigma-Aldrich, 97% by weight) which was stirred for 1 hour was added. Finally, it was added 0.7mL of deionized water as hydrolyzing agent that was 2 hours stirred. The resulting mixture was aged 7 days. The deposit of the films was performed by dipping or dip-coating, with immersion times of 1 minute and dried at 100°C during 1 hour. Plates were heated at 450°C at 3°C/minute and 4 hours in order to obtain a mixture of anatase and rutile phases. The synthesis of hydroxyapatite nanopowders was performed by controlled precipitation. Stoichiometric volume of 0.1M calcium nitrate tetrahydrate ($Ca(NO_3)_2{\cdot}4H_2O$, Sigma-Aldrich 99.2%) aqueous solution was added dropwise to 0.06M diammonium hydrogen phosphate ($(NH_4)_2HPO_4$, (Sigma-Aldrich 99.2%) aqueous solution. The solution was electromagnetically stirred, for continuous stirring, of the dispersed medium. During precipitation, the pH was monitored and adjusted at 10±0.1 by adding NaOH (Sigma-Aldrich). Meanwhile, sodium hydroxide (Sigma-Aldrich) was added immediately to adjust the pH reaction mixture. The pH value was kept constant throughout the experiment. After the addition, stirring was continued for 2 more hours, to homogenize the solution. The precipitate was aged for 3-9 days at room temperature, at rest. Finally, the coatings hydroxyapatite nanopowders were performed by dip-coating technique dipping the 304 stainless steel and Ti plates with $TiO_2$ coating solution within hydroxyapatite, after aging. The substrate was placed horizontally into the solution of HA for 2 hours, then extracted vertically and dried at room temperature for 12 hours, after that they were dried at 100°C for one hour and muffle calcined at 450ºC/ for 4h at 2.0°C/min with a dwell time of 2h.

### *2.2. Coated Powder Characterization*

The X-ray diffraction was performed on a D8 ADVANCE diffractometer (Bruker) with DAVINCI design, geometry theta - theta using monochromatic radiation of Cu tube and detector LINXEYE silicon. Preliminary tests were conducted to define appropriate difractional registration and field conditions. The analysis conditions were using a monochromator 0.02 NiO, collimator 0.2mm, step time 4s, 02 increases, and 15-90° difractional field. Identifying diffractograms was performed using the software DIFFRAC. EVA version 3. The morphologies of the samples were obtained using a field emission electron scanning microscope (FESEM) brand FEI QUANTA FEG model 650, with an acceleration voltage 10kV. To improve visualization of the carbon coating samples was performed on a computer model QUORUM Q R 15R. A detector for punctual EDS analysis was used to perform elemental chemical analysis. The analysis by micro-RAMAN spectroscopy was carried out with a team HORIBA Scientific LabRAM HR Evolution.

## 3. Results and discussion

### *3.1. Microstructural analysis*

The peaks obtained by wet chemical route for HA particles are shown in Figure 1. From Figure 1 HA, XRD pattern showed higher consistency with standard references in JCPDS file available in software for hydroxyapatite (09-0432). XRD pattern indicates that HA crystals were produced on stainless steel and Ti surface by wet chemical processes when taking no account of the stainless steel and Ti peaks. Some characteristic peaks of HA can also be observed at the angles of 26° and 30°–35°, which belong to the (002), (211), (112), and (300) diffractions. It is clear that there is an orientation growth of (002) plane in HA, which is consistent with the observation by other bioactive coatings [5].

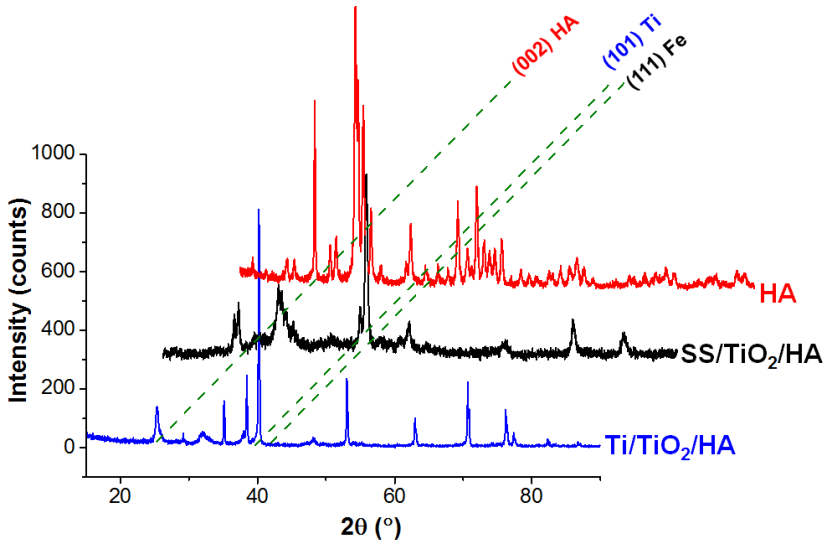


**Figure 1.** Growth hydroxyapatite (HA) coating on metal substrates (Stainless steel=SS and Titanium=Ti) with surface modified $TiO_2$ observed by XRD. The more intense peaks from HA (coating), Ti (substrate) and stainless steel (substrate) are highlighted in the graphic.

It is also found from Figure 1 pattern HA, that the diffraction peaks of (211), (112), and (300) planes are intensified going from titanium to steel. In pattern Ti/$TiO_2$/HA sample, the appearance of Ti reflections indicates that the coating deposited on the Ti substrate should be thin. Coatings showed a mixture of phases, the predominant phase in both cases, the reflections of higher intensity were anatase at the angles 26.9°, 39.3° and 49.7° which correspond to the (101), (112) and (202), respectively, in agreement with the crystallographic letter JCPDF 21-1272 and to a lesser extent is present in the rutile phase at the angles 28.7° and 37.6° corresponding to the (101) and (103) respectively, which coincide with the crystallographic letter JCPDF 29-1360. In the DRX pattern SS/$TiO_2$/HA sample, the presence of a peak (111) (2θ=43.1°) plane was detected and the signal at (200) (2θ=63.3°) indicates the presence of Fe in the γ-phase [6]. All the HA peaks were detected and indexed along with the iron peaks.

SEM images of HA coatings obtained on modified $TiO_2$ steel substrates (SS/$TiO_2$/HA) are presented in Figure 2. The images reveal considerable agglomeration among the particles, which increases the size of the crystalline powders. It also shows the morphology of the coatings of HA/$TiO_2$ deposited on steel at room temperature characterized by high density of microcracks in the coating of $TiO_2$, which could affect the uniform coating of HA growth. HA coating does not completely cover the steel substrate. In Figure 2, the $TiO_2$ coating areas with microarrays, porosity and formation of agglomerates were observed at the micrometer size. This morphology is well documented for $TiO_2$ thin coatings obtained by sol-gel [7].

Micrographic images of HA coatings obtained on modified $TiO_2$ titanium substrates (Ti/$TiO_2$/HA) are exhibited in Figure 3. The images reveal considerable agglomeration among the particles, which increases the size of the crystalline powders. It also shows the morphology of the HA/$TiO_2$ coatings deposited on titanium at room temperature characterized by high density of microarrays in HA coating, which may be related to microarrays in the coating of $TiO_2$ prepared by sol-gel which could affect the uniformity of HA growth coating. HA coating does completely cover the $TiO_2$ substrate coating areas with microarrays, porosity and formation of agglomerates were observed at the micrometer size.

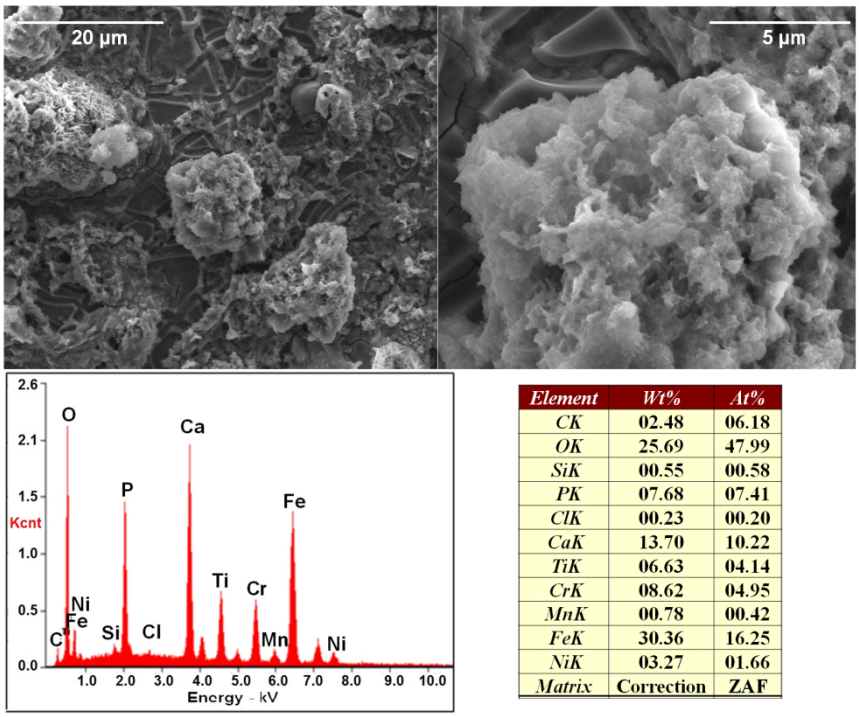


| Element | Wt% | At% |
|---|---|---|
| CK | 02.48 | 06.18 |
| OK | 25.69 | 47.99 |
| SiK | 00.55 | 00.58 |
| PK | 07.68 | 07.41 |
| ClK | 00.23 | 00.20 |
| CaK | 13.70 | 10.22 |
| TiK | 06.63 | 04.14 |
| CrK | 08.62 | 04.95 |
| MnK | 00.78 | 00.42 |
| FeK | 30.36 | 16.25 |
| NiK | 03.27 | 01.66 |
| Matrix | Correction | ZAF |

**Figure 2.** SEM images of hydroxyapatite (HA) coating on metal substrate steel=SS with surface modified $TiO_2$. EDS analysis of hydroxyapatite coated. Table shows EDS analysis of the atomic % of Ca, P and O and other elements present in the powders Ca/P=1.38).

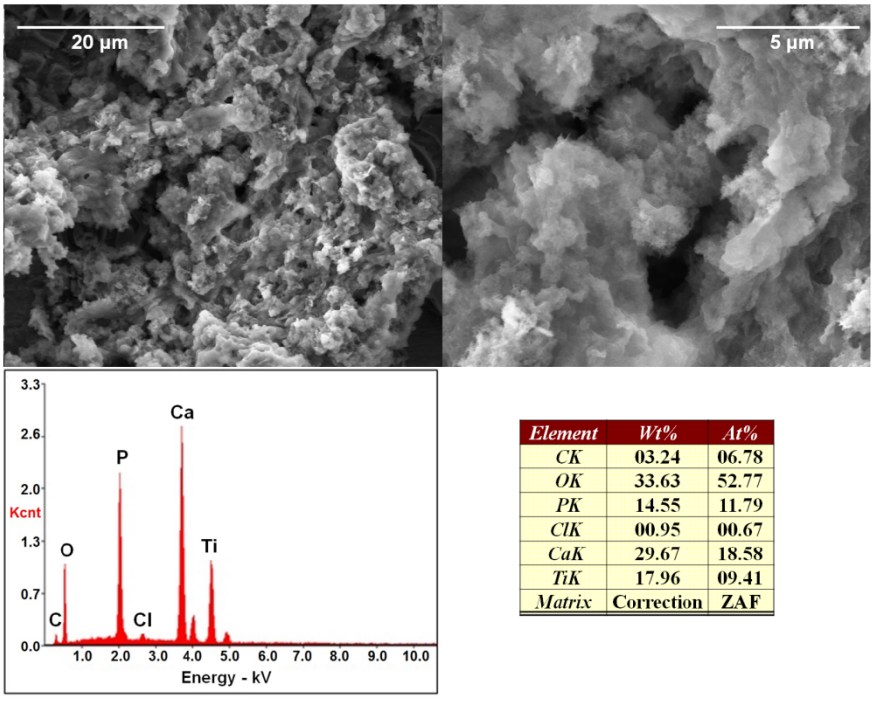


| Element | Wt% | At% |
|---|---|---|
| CK | 03.24 | 06.78 |
| OK | 33.63 | 52.77 |
| PK | 14.55 | 11.79 |
| ClK | 00.95 | 00.67 |
| CaK | 29.67 | 18.58 |
| TiK | 17.96 | 09.41 |
| Matrix | Correction | ZAF |

**Figure 3.** SEM images of hydroxyapatite (HA) coating on metal substrate Titanium=Ti with surface modified $TiO_2$. EDS analysis of hydroxyapatite coated. Table shows EDS analysis of the atomic % of Ca, P and O and other elements present in the powders. (Ca/P=1.58).

Coating the titanium substrate with $TiO_2$, the crystallinity of the HA coating increased, the structure became more compact and the Ca/P ratio increased due to the loss of P in the films. The addition of sodium hydroxide (to adjust the pH to 10) can increase the HA content in the coating. XPS and EDS outcomes for steel substrate and titanium showed poor calcium content as measured by a Ca/P ratio of 1.38 and 1.58, respectively, this composition is similar to that of natural apatite.

The Raman spectrum of HA coating is shown in Figure 4. The spectrum shows four distinguishable groups of spectral bands are evident. The first group consists of two bands at ~427.32 and ~443.15$cm^{-1}$. These bands correspond to the factor group splitting of the doubly degenerated bending mode $\nu_2$ of the $PO_4$ group (O-P-O bond). The bands at ~575.62, 586.76 and 604.57$cm^{-1}$ belong to the $\nu_4$ triply degenerated bending mode of the $PO_4$ group. The phosphate symmetric-stretch peak was observed in the range of 958.41$cm^{-1}$ which is characteristic for hydroxyapatite [8]. The very intense band at 958.41$cm^{-1}$ arises from the symmetric stretching modes and is designated as $\nu_1$ fundamental vibrational mode. The bands comprising the fourth group arise from the $\nu_3$ and are due to the asymmetric stretching vibrations of the P–O bonds these bands are seen at ~1026.80, 1043.84 and 1073.56$cm^{-1}$. In Figure 4, it can be seen that Ti/$TiO_2$/HA has a lower signal intensity at 958.41$cm^{-1}$ compared with the result in SS/$TiO_2$/HA at 956.26$cm^{-1}$, which could be due to a low adhesion material on the substrate modified $TiO_2$. In addition, anatase phase signals at 137.99, 391.04, 512.97 and 633.44$cm^{-1}$ were evident. The slight displacement of the signals obtained with respect to literature, indicates the presence of other calcium phosphate phases in the microstructure of the synthesized coating.

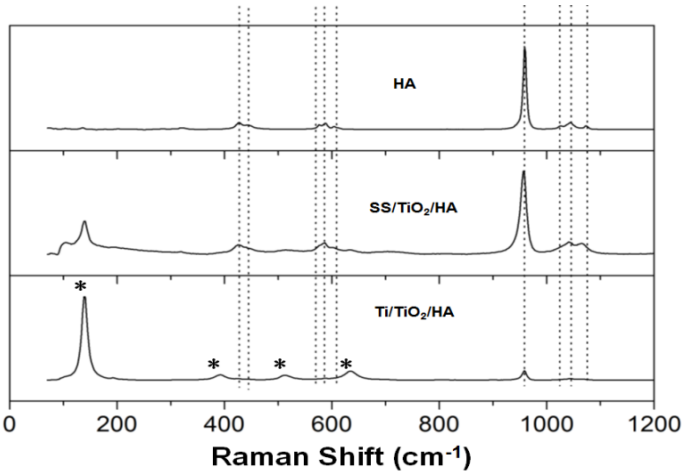


**Figure 4** Raman shift spectra of hydroxyapatite (HA) coating on metal substrates (Stainless Steel=SS and Titanium=Ti) with surface modified $TiO_2$. The dashed line shows the signals corresponding to hydroxyapatite powder. The asterisk indicates signals corresponding to coated titanium.

## 4. Conclusions

HA bioceramic was synthesized using ammonium dihydrogen phosphate and calcium nitrate by simple precipitation, sol-gel, and dip-coating methods approach. XRD, XPS, FESEM-EDS and Raman results suggest the presence of crystalline phases in HA particles after calcination at 450°C. The microstructure of hydroxyapatite coating depends mainly of the aging time and the base used to adjust the pH, and substrate material parameters. The ability to generate crystalline HA coatings combined with the low temperature used, render the precipitation, sol-gel, and dip-coating approach favorable for generating HA coatings on different metallic substrates modified with sol-gel $TiO_2$ coatings for biomedical applications.

**Acknowledgments**
Authors would like to thank the University Santiago de Cali for the financial support given to the Project DGI-COCEIN-No. 939-621115-N21. Authors also thank the Center for Corrosion Research (CICORR) of the Autonomous University of Campeche and the Center for Materials and Nanoscience (CMN) for providing necessary facilities.

**References**
[1] Jaffe W L, Scott D F 1996 *J Bone Joint Surg Am* **78(12)** 1918
[2] Furlong R J, Osborn J F 1991 *J Bone Joint Surg B* **73**(**5**):741
[3] LeGeros R Z 1991 *Monogr Oral Sci* **15** 1
[4] Wang C, Karlis G A, Anderson G I, Dunstan C R, Carbone A, Berger G, Ploska U, Zreiqat H 2009 *J. Biomed. Mater. Res. Part A* **90** 419
[5] Cameron H U, Macnab I, Pilliar R M 1977 *J Biomed Mater Res*. **11(2)** 179
[6] Zhang L, Li H, Li K, Zhang S, Fu Q, Zhang Y, Liu Shoujie 2015 *Ceramics International* **41**(**1**) 427
[7] Nik N, Che I, Yusairie M and Norjanah Y 2012 *APCBEE Procedia* **3** 46
[8] Torres F J, Panyayong W, Roger W, Velasquez-Plata D, Oshida Y, Moore B K 1998 *Biomed Mater Eng* **8** 25
[9] Szalkowska E, Gluszek J 2003 *Material Science* **21(4)** 367
[10] Smeulders D E, Wilson M A, Armstrong L 2001 *Ind Eng Chem Res* **40** 10